



ELSEVIER

Available online at www.sciencedirect.com

SCIENCE @ DIRECT®

Nuclear Instruments and Methods in Physics Research A 499 (2003) 24–44

**NUCLEAR
INSTRUMENTS
& METHODS
IN PHYSICS
RESEARCH**
Section Awww.elsevier.com/locate/nima

Magnet system for the KEKB main ring

Kazumi Egawa, Kuninori Endo, Hitoshi Fukuma, Tadashi Kubo,
Mika Masuzawa, Yasunobu Ohsawa, Norihito Ohuchi, Toshiyuki Ozaki,
Kiyosumi Tsuchiya, Masato Yoshida, Ryuhei Sugahara*

Accelerator Laboratory, High Energy Accelerator Research Organization (KEK), Oho 1-1, Tsukuba-shi, Ibaraki 305-0801, Japan

Abstract

KEKB is a two-ring electron–positron collider with asymmetric energies of 8 and 3.5 GeV to study CP violation in B meson decay. In KEKB, there are 21 types of magnets; about 1600 in total. About 430 dipole and quadrupole magnets were recycled from TRISTAN, the preceding program. All quadrupole magnets are equipped with vertical and horizontal steering dipole magnets. The number of steering magnets is about 1700. There are 212 sextupole magnets, and all of them are fixed on remotely controlled movers to adjust their positions to the beam passage. All main dipole magnets have back-leg coils to steer beams precisely. All quadrupole and sextupole magnets are equipped with correction coils to have a capability for beam-based alignment. Also one-turn coils are installed as well to each magnetic pole of the main magnets to monitor the magnetic flux in the case of trouble. The magnetic field in all magnets was measured and its quality strictly checked. After field measurement, the magnets were installed and precisely aligned. A cooling water system and a power supply system for these magnets were constructed. Magnet design was started in 1994, and construction of the two rings was completed in November 1998. The parameters of the magnets and the construction of the KEKB magnet system are described. Some of the problems experienced during this construction work are also presented.

© 2002 Elsevier Science B.V. All rights reserved.

PACS: 29.20

Keywords: B-factory; Magnet; Magnetic field measurement; Power supply; Alignment

1. Introduction

KEKB is a two-ring electron–positron synchrotron collider with asymmetric energy (8 GeV for electrons and 3.5 GeV for positrons) [1] for experiments on CP violation in B-meson decay [2]. These two rings were constructed in the same

accelerator tunnel as that for the preceding TRISTAN program [3].

Design of the magnets was started in 1994, and the first lot was ordered in 1995. The actual construction work of the two rings in the tunnel was started in January 1996, soon after terminating the TRISTAN operation at the end of December 1995. After the construction of the two rings was accomplished in November 1998, the commissioning of electron beams was started in early December.

*Corresponding author.

E-mail address: sugahara@post.kek.jp (R. Sugahara).

The variety and number of magnets for KEKB are large. There are 21 types of magnets, and about 1600 in total. Out of these magnets, 119 dipole and 314 quadrupole magnets were recycled from TRISTAN magnets. All of the quadrupole magnets are equipped with horizontal and vertical steering dipole magnets. Their number is about 1700 in total. Each magnetic pole of all quadrupole and sextupole magnets is equipped with correction coils and one-turn coils. One-turn coils are installed in the main dipole magnets as well. The correction coils are to have a capability of beam-based alignment, and the one-turn coils are used to monitor the magnetic flux in each pole in the case of trouble.

The magnet system for the KEKB main ring, including power supplies and the cooling water system, is described, except for two superconducting final focusing magnets and six special IR quadrupole magnets, which are described in the article “Interaction Region (IR)”. Also the handling (i.e. the magnetic field measurement, installation and alignment) of such a large number of magnets is described as well.

2. Magnets

The design of the magnets for the positron Low-Energy Ring (LER) was started in 1994. We then proceeded to designing magnets for the electron High-Energy Ring (HER) while taking into account reuse of the TRISTAN magnets. The first batch of the LER magnets was ordered in July 1995, and the final delivery was made in March 1998.

In order to achieve low emittance and high luminosity, high precision in the magnetic field is required, as shown in Table 1. To realize this high precision, silicon steel, the material used for laminated magnet bodies, is required to satisfy severe tolerances, as shown in Table 2.

There are 167 (125) main dipole magnets, 458 (448) quadrupole magnets, 108 (104) sextupole magnets and 152 (0) wiggler magnets in the LER (HER); 40 more wiggler magnets may be added in

Table 1
Tolerances for systematic multipole errors

Type of magnets	Tolerance at 50 mm radius (%)
Dipole magnets	$B_3/B_1 < 0.12$ $B_5/B_1 < 0.45$
Quadrupole magnets	$B_6/B_2 < 0.12$ $B_{10}/B_2 < 0.14$

Table 2
Tolerances for magnetic property of silicon steel. B_{50} and $H_c^{1.5}$ stand for the flux density at $H = 5000$ A/m and the coercive force at excitation of $B = 1.5$ T, respectively

$B_{50} > 1.6$ T	$\Delta B_{50}/B_{50} < \pm 1\%$
$H_c^{1.5} < 70$ A/m	$\Delta H_c^{1.5}/H_c^{1.5} < \pm 5\%$

future. The total number of these main magnets is about 1600, including spare magnets, and the number of varieties is 10 for the LER and 13 for HER. Each quadrupole magnet is equipped with vertical and horizontal steering dipole magnets. The total number of steering dipole magnets is about 1700. The vertical steering dipole magnets were designed and fabricated at IHEP, Beijing, and the horizontal ones at BINP, Novosibirsk, under cooperative research between KEK-IHEP and KEK-BINP, respectively. The parameters for the LER and HER magnets are listed in Tables 3 and 4, respectively, and those for the LER and HER steering dipole magnets in Tables 5 and 6, respectively. Fundamental guide lines in the design and fabrication are listed as follows:

- (1) The electric current should be small to reduce the size of power cables.
- (2) The transverse dimension of the magnets should be as small as possible, because the distance between the LER and HER is tight. The distance between the two rings ranges from 1.0 to 1.2 m.
- (3) In order to achieve high precision in the magnetic field, special attention should be paid to fabrication errors in the shape and length of the magnetic poles, and to those in the air gap as well. Special attention should

Table 3
LER magnet parameters

Type	$g/2$ or r_B (mm)	L_{lam} (m)	B, B', B'' (T, T/m, T/m ²)	No. of mag.	$I \times$ turns /pole	Comments
B	57 (54)	0.76	0.848	134+1	1250A \times 32	
Blc	57 (55)	2.1	0.52	26	1000A \times 24	Local corr.
BV	55	1.2	0.2	4	500A \times 18	Vertical cross. at Fuji; block
BS	57 (54)	0.3	0.21	3	500A \times 20	Weak B; block
BC1LP	92.5 (82.5)	0.2	0.032	1	5A \times 1008	H-shape
BC2LP	105 (100)	0.2	0.045	2	4.2A \times 1024	= LER-StVW
BC3LP						
Wigg	55	0.75	0.77	152+2 +(40)	944.4A \times 36	Wiggler
QA-I	55	0.4	10.2	284	500A \times 25	
QA-II	55	0.4	10.2	129+3	500A \times 25	
Qrf	83	0.5	6.32	37+5	500A \times 35	RF section
Qk	105	0.2	0.73	8+1	200A \times 16	Skew Q
SX	56	0.30	340	104+2	425A \times 21	F-/D-type
SxC	85	0.50	77.5	4+1	425A \times 21	F-/D-type

Values in parenthesis are the smallest gap sizes at the edge of the gap. Second number in fifth column is a number of spares.

Table 4
HER magnet parameters

Type	$g/2$ or r_B (mm)	L_{lam} (m)	B, B', B'' (T, T/m, T/m ²)	No. of mag.	$I \times$ turns / pole	Comments
B	35 (33.15)	5.804	0.30	117+2	840A \times 10	Recycled
BS1	35 (33.15)	2.8	0.048	6	10A \times 150	Weak B, recycled
BsFL	35 (33.15)	1.14	0.214	1	500A \times 12	Weak B, recycled
BsFR	57 (54)	0.76	0.339	1	500A \times 32	Weak B, = LER-B
BHL	95 (86)	0.2	0.0745	1	5A \times 1152	= HER-StHW
BC1LE	90 (80)	0.25	0.070	1	5A \times 1008	H-shape
BC2LE	105 (95)	0.20	0.058	2	5A \times 1008	H-shape
BC2RE						
BC1RE	105 (95)	0.34	0.060	1	5A \times 1008	H-shape
BC3LE	105 (100)	0.2	0.08	1	4.2A \times 1792	= HER-StVW
QA	50	0.762	8.5	199+2	500A \times 17	Recycled
QB	50	0.95	8.5	110+3	500A \times 17	Recycled
QS	50	0.5	12.7	80+2	500A \times 26	
QX	50	0.76	12.7	4+1	500A \times 26	
Qrf	83	1.0	6.32	43+1	500A \times 35	RF section
Qk1	80	0.3	1.25	5+1	200A \times 16	Skew Q
Qk2	105	0.5	0.73	7+1	200A \times 16	Skew Q
SxF	56	0.3	340	56	425A \times 21	F-type; = LER-SX
SxD	56	1.0	348	48+1	425A \times 21	D-type

Values in parenthesis are the smallest gap sizes at the edge of the gap. Second number in fifth column is a number of spares.

also be paid to the precision of the flatness and tilt of the fiducial bases and the position and diameter of the target holding holes on each magnet.

(4) Low current density in the coils and much cooling water flow are preferable to keep the temperature rise low and the magnetic field drift small.

Table 5
LER steering dipole magnet parameters

Type	$g/2$ or r_B (mm)	L_{lam} (m)	BL_{eff} (Tm)	No. of mag.	$I \times$ turns / pole	Comments
StV	80 (76.5)	0.2	0.0198	413 + 7	4.2A \times 896	
StVW	105 (100)	0.2	0.0179	38 + 3	4.2A \times 1024	RF sect.
StH	64 (58)	0.2	0.0128	385 + 7	5A \times 400	
StHW	95 (86)	0.2	0.0127	21 + 4	5A \times 500	RF sect.
StHWX	105 (100)	0.2	0.0179	6 + 1	4.2A \times 1024	= HER-StVW

Values in parenthesis are the smallest gap sizes at the edge of the gap. Second number in fifth column is a number of spares.

Table 6
HER steering dipole magnet parameters

Type	$g/2$ or r_B (mm)	L_{lam} (m)	BL_{eff} (Tm)	No. of mag.	$I \times$ turns /pole	Comments
StV	80 (76.5)	0.2	0.0310	391 + 9	4.2A \times 1408	
StVW	105 (100)	0.2	0.0309	43 + 6	4.2A \times 1792	RF sect.
StH	40 (36.5)	0.2	0.0286	353 + 7	5A \times 648	
StHW	95 (86)	0.2	0.0287	44 + 5	5A \times 1152	RF sect.
StHW	95 (86)	0.2	0.0287	44 + 5	5A \times 1152c	RF sect.
StV-HX	80 (70)	0.2	0.0782	2	5A \times 1008	H-shape

Values in parenthesis are the smallest gap sizes at the edge of the gap. Second number in fifth column is a number of spares.

- (5) Correction coils are installed in the main quadrupole and sextupole magnets, except for the skew quadrupole magnets, so as to have the capability of beam-based alignment. Back-leg coils are installed in the main dipole magnets for the fine steering of beams.
- (6) One-turn coils are also installed on each pole in the main dipole, quadrupole, sextupole and wiggler magnets to monitor the magnetic flux for each pole in the case of trouble.
- (7) Sufficient space should be given to adjustment work for the horizontal and vertical position of magnets.
- (8) Newly fabricated magnets are supported on three points to make vertical position adjustment easy.

The number of the TRISTAN magnets, which were refurbished and used as HER main magnets, was 119 for the dipole and 314 for the QA and QB quadrupole magnets. The outer shielding layer of the coils for the dipole magnets were renewed. The back-leg coils were also renewed. Correction coils

and one-turn coils were newly installed to each magnetic pole of the QA and QB quadrupole magnets. The surface of the fiducial bases which rusted or had scratches were re-polished. A small number of fiducial bases on quadrupole magnets needed special treatment, because the surfaces of some bases were damaged or other bases exceeded the mechanical tolerances by three times or more. The surfaces of these bases were chipped off by 5 mm, new plates were bolted on, and the surfaces were then machined so as to satisfy the mechanical tolerances. Also, because the end shims used to adjust the shape of magnetic field had rusted, all of them were replaced by new ones.

3. Remotely controlled movers

Most of the KEKB quadrupole magnets are equipped with vertical and horizontal steering magnets as well as beam position monitors. Deviation of the beams from the center of the quadrupole magnets is detected by beam position

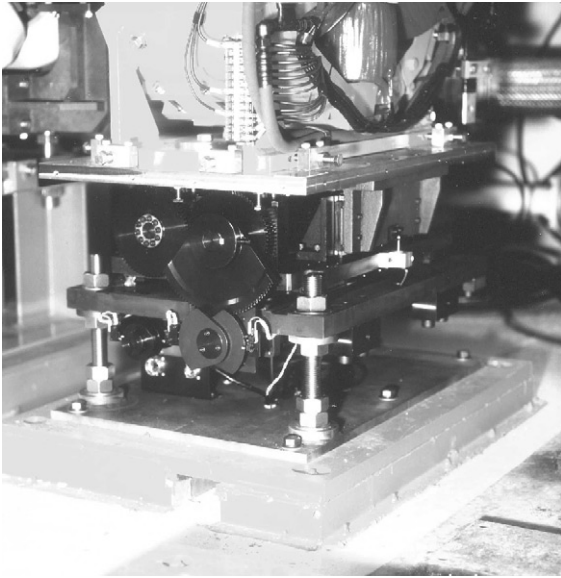


Fig. 1. A picture of one of the movers for the sextupole magnets.

monitors; this deviation is corrected by steering magnets. To correct for deviation of the center of the sextupole magnets from the beams, positions of the sextupole magnets are adjusted by movers. Because there are three kinds of sextupole magnets, the variety of magnet movers is also three. There are 212 movers in total. Fig. 1 shows a picture of one of these sextupole magnet movers.

Magnet movers have a capability of both coarse adjustment and precision adjustment. The coarse adjustment is performed by pushing magnets by screw bolts in three directions. There are three bolts used to support the weight of the magnets. Three-bolt support is convenient to adjust the vertical position, because there is no extraneous bolt. The range of the coarse adjustment is ± 20 mm.

In the precision adjustment, horizontal movement (X movement) is performed by rotating ball screws using stepping motors. The movement is guided by precision Linear Motion (LM) guides. The movement is only along the direction perpendicular to the beam. The vertical movement (Y movement) is performed by cam movers [4]. The cam shaft has an offset of 3 mm from the shaft rotated by a stepping motor. A magnet is mounted on a cam shaft and it is moved vertically because

of the offset as the shaft rotates. Y , the vertical position of the magnet, is expressed as $Y = d \sin \theta$, where d and θ stand for the offset of the cam shaft and the rotation angle measured from the horizontal axis, respectively. In order to support the heavy weight of magnets, ranging from 1.2 to 2.0 t, inserts are installed between the cam shafts and the magnets. Inserts contact with the cam shaft through surrounding ball bearings, and with the magnet through a short LM guide installed in the transverse direction to the rotation axis of the shaft. If a magnet is mounted directly on the cam shaft at line contact, the cam shaft might be broken because its surface is brittle. In this way, the magnet is moved up and down, but it can move freely in the horizontal direction along the short LM guides. Therefore, the vertical movement is guided by vertical LM guides and the horizontal movement is restricted so as to maintain the horizontal position of the magnets and to make free the horizontal movement of the center of the cam shaft. The range and the precision are required to be ± 2 mm and $10 \mu\text{m}$, respectively. The actual precision achieved was about $4 \mu\text{m}$. The error is introduced by a backlash in the movement. The distortion of the mover system caused by the installation error of LM guides is responsible for this backlash. The speed of the movers is comparatively fast, 0.13 mm/S for the horizontal movement and $0.13 \cos \theta \text{ mm/S}$ for the vertical movement.

To monitor the positions of the magnets, each mover is equipped with two Linear Variable Differential Transformers (LVDTs): one is for the X movement and the other for Y movement. Their range and speculated precision are ± 3 mm and $10 \mu\text{m}$, respectively. An actual precision of $4 \mu\text{m}$ is obtained within a range of ± 2 mm.

The magnet movers are connected to mover control modules scattered in eight Local Control (LC) huts along the circumference of the accelerator ring and in the D2 Power Supply (PS) control room as well. Each LC hut can handle 26 movers located in the corresponding area of the ring tunnel; the D2 PS control room handles four movers for the SxC magnets located in the Tsukuba straight section. Movers receive a train of driving pulses for stepping motors from mover

control modules, and send the output from LVDTs and the status signals of X and Y limit switches to them. LVDT signals are converted to current signals and fed to a data logger in each control hut. The data logger can handle up to 60 signals. The data logger controlled in the GPIB mode is connected to a VME-GPIB interface module in a VME subrack. The Input/Output Controller (IOC VME single board computer) installed in the VME subrack communicates with mover control modules in each control hut through a serial bus and also with the central computer through the KEK network system. Commands and data are transferred from the central computer to mover control modules through IOCs; the status of each X and Y limit switch is transferred reversely. The LVDT signals are digitized by data loggers, read by IOCs and sent to the central computer. The mover control software is built within the framework of EPICS [5], the software code adopted for KEKB accelerator control.

4. Cooling water system

The coils of the magnets, except for some small magnets, steering magnets and correction coils, are made of a hollow conductor. These coils are cooled by neutralized water flowing through the conductor. There are four magnet cooling water stations located near to the TRISTAN experimental buildings, Tsukuba, Oho, Fuji and Nikko. Each cooling water system covers the left and right areas of each experimental hall. The cooling water system consists of three water pumps (one of them is usually at rest as a spare) and a cooling tower, where the water is cooled down by exchanging heat between the water and the air. The temperature is controlled by bypassing the cooling tower. The rate of bypassing water is controlled by a cross valve. About 2% of the whole flow is led to an ion-exchange resin tank and neutralized. The magnet cooling water systems can supply water at a rate of up to 3660, 3660, 4020 and 3860 l/min in the Tsukuba, Oho, Fuji and Nikko areas, respectively. The water pressure is 12 and 3 kg/cm² at the inlet and outlet of the magnet, respectively.

The water flow is controlled in a constant output pressure mode. Only in Nikko was the operation mode changed in the summer of 2000 to a constant pressure difference mode, which keeps the difference constant between the water pressure at the pump output and that at the return from the tunnel (not at the pump inlet). Under constant pressure operation, the water flow has a seasonal variation of about 5% at most because the rate of bypassing water changes according to the air temperature, and conductance of the bypassing route and that of the cooling tower route are different. It was proved by changing of the operation mode at Nikko that the constant pressure difference mode can really keep the water flow constant regardless of the air-temperature variation. The whole system will be changed to the constant pressure difference mode in the near future.

In the tunnel, there are 96 connection points, each of which is equipped with two main valves, one for the inlet and the other for the outlet. The cooling water is distributed from these connection points to about 1600 main magnets. At each magnet a flow-control globe valve and a strainer are installed at the inlet, a diaphragm-type flow switch at the outlet and bimetal-type temperature switches on each coil. A strainer prevents dust from flowing through. The flow switch and the temperature switch protect coils against overheating by sending out interlock signals. The material for spindles of water flow switches was changed from brass to SUS-304 based on experience at TRISTAN. It was found that part of the spindles, which made an adjustable gap for the water flow and produced the pressure difference, were eroded when some of them were opened after terminating the 9-year TRISTAN operation. Also, some spindles of the same type flow switches were found to be eroded by as much as 0.4 mm in 1 year in the PF-AR ring (which was previously the TRISTAN accumulation ring). Although a globe valve is usually used as a stopping valve, it is much cheaper than a needle valve. It was therefore tested on a test stand to control water flow using the globe valves. It was found that they worked well to adjust the magnet cooling water flow. The cooling water flow in the magnet coil was designed for the

temperature rise of water to be less than 15°C, except for a small number of magnets, in which the small conductance forces the water temperature rise slightly higher than 15°C. In order to adjust the opening of the globe valves and the interlock level of the water flow switches, the water flow is measured at the straight section of outlet pipes by a portable supersonic flow-meter, LT868 of Japan Panametrics.

Two main problems are discussed in the following. One is clogging inside the hollow conductor. A power supply was shutdown by the coil temperature interlock for B2P.55 (an LER-B type magnet) on December 1, 1998. It was found in a following investigation that epoxy resin sneaked into some of the coils during a dipping process of insulated coils into the epoxy resin bath. For each LER-B type magnet, the inside of the inlet and the outlet of the coils was carefully observed by an optical fiber scope. L-shaped inlets and outlets were cut off when some epoxy resin was found, and the insides of the coils were observed by inserting the optical fiber scope further. After all, the insides of about 10% of the coils for LER-B magnets had to be cleaned by a solvent in the tunnel during the winter shutdown period. The other problem is frequent interlock signals from water flow switches for all types of magnets. Before the summer shutdown in 2000, about 50 power supplies were turned off within 2 months because of water flow interlocks. Many air bubbles had been observed in the pipe, especially in the high-pressure side. Someone thought these air bubbles caused the fluctuation of water flow which resulted in interlocks. During the summer of 2000, the air-evacuation system was improved by installing air-collecting tanks at the top of pipes which go down to the tunnel. The air-collecting tanks are equipped with automatic air-evacuation valves. No air bubbles have been observed since then, except for in the Fuji area, where some very small bubbles still remain in both the high- and low-pressure sides. Almost for 1 year, there has been no breakdown of the magnet power supplies caused by the water flow interlock, except for one, which was caused by the miss-adjustment of a control valve.

5. Magnetic field measurement

The magnetic fields in all magnets were measured to check their quality. Four types of measuring equipment were used: flip coil type, harmonic coil type, rotating coil type and Hall probe type.

The magnetic field for the LER wiggler magnets, the HER-B magnets and the steering dipole magnets were measured at the place of fabrication. The other magnets were measured at KEK on the basement floor of the Nikko experimental hall. In order to acquire a precision in the field measurement as high as 1.0×10^{-4} , the environment of the hall had to be improved. The air conditioner was adjusted to keep the air-temperature fluctuation less than 1°C, and the direction of the wind was adjusted so as not to blow directly on the field measuring equipment. The cooling water supply was also adjusted so as to keep the fluctuation of the water inlet temperature less than 0.1°C.

The magnetic field in the dipole magnets, except for the LER-BV magnets, is measured by flip coils. An analog output is fed to a Metrolab high precision integrator (PDI5025). The measuring system is controlled and the data are recorded by software on a stand-alone personal computer. The long flip coil measures BL, the field strength integrated along the Z-axis (beam axis). Mapping of the magnetic field along the Z-axis is performed by short twin flip coils for at least one magnet of each type. A twin coil is used for dipole magnets, and for quadrupole and sextupole magnets as well. The mapping results provide information on the effective length of the field (L_{eff}). The mapping twin coils were calibrated at the center of the reference dipole magnet, where the absolute field strength is measured by NMR equipment. The long flip coil system is then calibrated by comparing the measuring results with those from the mapping twin coils. The harmonic coils are calibrated in the same way by measuring the field in the reference dipole magnet. The magnetic field in quadrupole and sextupole magnets and that in LER-BV magnets are measured by harmonic coils. The analog output is measured by the Metrolab integrator (PDI5025). The measuring system is controlled by an IOC installed in a VME subrack

placed on the Nikko basement floor. Measuring data and the status of the field measuring equipment are read and sent to a central computer by the IOC. The IOC communicates with the central computer through the KEK network system, and with the field measuring equipment through a VME-GPIB interface module installed in the VME subrack. The control software is built in the framework of EPICS. The operation is performed on an X-terminal in the Nikko experimental hall. The X-terminal communicates with the central computer through the KEK network system. The harmonic coil system for the LER magnets has four coils: a long coil to measure the integrated magnetic field (BL , $B'L$ or $B''L$), and three short coils to obtain information about the effective length of the field (L_{eff}), and the transverse offset of the field center (ΔX and ΔY) from the center of the measuring system (mechanical center). The other two harmonic coil systems have another coil, the bucking coil, to measure the field precisely by canceling the main component. The angle (θ_{med}) between the median plane of the field and the horizontal axis (X -axis) of the measuring system is measured as well. A 2.5 m long harmonic coil is used to investigate the magnetic coupling between quadrupole and steering dipole magnets placed near by. The magnetic field in the wiggler magnets is measured by a rotating coil system, which has a long coil and two half-length coils. The long coil measures BL . Because the direction of the field is flipped at the center of the magnet, this measurement results in residual field. The half-length coils measure BL for each pole. The analog output is analyzed by a spectrum signal analyzer (HP3562A). The magnetic field in the vertical steering dipole magnets was also measured by a rotating coil system at IHEP, Beijing. That in the horizontal steering dipole magnets was measured by a Hall probe system at BINP, Novosibirsk. The magnetic field measuring equipment used is summarized in Table 7.

The magnetic field mass measurement was conducted during a period of about 18 months from January 1997 to June 1998. During this period the magnetic measurement was performed soon after delivery of the magnets in order to feed

back information to the fabricating factories. On the way, some problems were found [6]. One is a local shortage in a coil for HER-QS, which can be seen as an abnormal amplitude for the main component ($n = 2$, where n stands for the number of multipole) and $n = 6$ allowed component, as shown by the solid circles in Fig. 2. This magnet was returned to the factory and the coil was replaced by a new one. The change in the permeability of the metal material also caused problems. The quadrupole amplitude distribution for the LER-Qrf magnets shows three peaks at the maximum excitation of 500 A. This is caused by a lot-by-lot change in the permeability of silicon steel, the material used for laminated cores. Although the standard deviation for the whole distribution is well within the tolerance, only members in the same group are connected to the same power supply. Another problem occurred in the LER-QA magnets. The LER-QA magnets are classified into two groups, QA-I and QA-II, according to the fabrication place. Although the specifications for QA-I and QA-II are the same, the QA-I and QA-II magnets show different field strength. This is caused by the small, but nontrivial, permeability of the SUS-304 pole end plate in the QA-I magnets. Thus, the magnets in these two groups cannot be mixed up in connecting to power supplies. The field strength for the sextupole magnets (LER-SX and HER-SxF) changed on the way. The change occurs around the production number 40. It was revealed that the punching die was modified around this production number. Because all sextupole magnets are paired, the partner is selected so as to keep the difference in the magnetic field strength less than 5×10^{-4} . A big problem is caused by hysteresis in the recycled quadrupole magnets. The recycled TRISTAN quadrupole magnets had been excited at a maximum current of 1500 A, and those are powered by 500 A power supplies at KEKB. Some of these had been used as focusing lenses (F-type) and the others as defocusing lenses (D-type). During a magnetic field measurement, they are connected to a power supply as F-type, and two peaks are observed in the amplitude distribution for the main component, as shown in Fig. 3. This is caused because the TRISTAN magnets had been

Table 7
Magnetic field measuring equipment

Type	Usage		L_{coil} (mm)	Diam. (mm)	Turn	Measured	Place
Flip coil	Short B no. 1		2000	19.3	4	LER-B,BS; HER-BsFR	KEK
	Short B no. 2		3600	15	2	LER-Blc; HER-BS BsFL	KEK
	Long B		6600	15	2	HER-B,	Co. M
		Separation (mm)	H_{coil} (mm)	$D_{\text{out}}/D_{\text{in}}$ (mm)			
Short twin flip coils	Mapping	~ 10	12	8.0/2.7	2090	B, Q, Sx, Wigg	KEK
		Comment	L_{coil} (mm)	$R_{\text{out}}/R_{\text{in}}$ (mm)			
Harmonic coil	For LER mag.	Main	1500	50.0/0.0	1	LER-QA, Qrf,Qk SX, SxC; HER-Qk1	KEK
		Side short	2 × 300	42.2/0.15	2	Qk2, SxF	
		Center short	200	42.2/0.15	2	HER-QA,	KEK
	For HER mag.	Main	1800	46.5/0.0	1	QB,Qrf,QS	
		Side short	2 × 600	40.3/1.3	1	QX,SxD;	
		Center short	200	40.3/1.3	1	LER-BV	
		Bucking	1780	34.9/11.6	2	Q - St	KEK
	For Q-St coupling	Main	2500	45.0/0.0	1		
		Side short	2 × 600	37.8/1.3	1		
		Center short	200	37.8/1.3	1		
	Bucking	2480	33.8/11.25	2			
Rotating coil	For wiggler	Long	1500	43.6/0.2	1	LER-Wiggler	Co. T
		Half L	748.6	43.7/0.5	1		
	For St-V	Main	870	51.3/–36.5	16	Verti. St	IHEP
		Bucking		36.5/–5.13			
Hall probe	For St-H					Hori. St	BINP

removed without any demagnetization, and thus each magnet remembers its hysteresis. An alternating excitation between currents of +500 and –500 A cannot solve this problem. Thus, the TRISTAN F- and D-type magnets are not mixed up, but are connected to different power supplies. The magnetic coupling between the quadrupole magnets and the steering dipole magnets placed near by have been studied [7]. This study is important because the smallest separation between a quadrupole magnet and a steering one is about 200 mm in the tunnel. The effect of the back-leg

coil excitation to the main dipole field has also been studied [8].

One magnet for each type is assigned as a reference magnet. The reference magnet and the magnet to be measured are placed face to face in the case of dipole magnets. The measuring equipment is placed between the two, and a measuring probe can be moved into the pole gap of the magnet to be measured, and then into that of the reference magnet, because the dipole magnets for KEKB are of the C-type. At the end of every measurement the magnetic field for the

reference magnet is measured, and the measuring results for the magnet to be measured are normalized to eliminate drift in the measuring system. In the case of the quadrupole or sextupole magnets, the magnetic field for the reference magnet is measured every 10 days to check whether there is any drift or errors in the measuring equipment.

BL , the magnetic field integrated along the Z-axis, is measured at various currents. Also the change in BL along the X-axis ($BL(X)$) is measured as well for the dipole magnets to see

whether a good field region of ± 50 mm in the X-direction is realized. Information on the amplitude for higher order components is also obtained from this $BL(X)$ measurement. The results of the magnetic field measurements are summarized in Table 8 for the dipole and wiggler magnets, and in Tables 9 and 10 for the quadrupole and sextupole magnets, respectively. The standard deviations for the distribution of the integrated main component (BL , $B'L$ or $B''L$) and L_{eff} for each type of magnet are sufficiently small. The pole-end shim-correc-

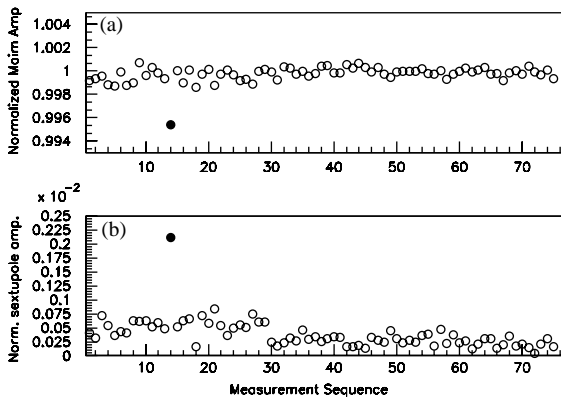


Fig. 2. (a) Normalized main amplitude and (b) normalized sextupole component are plotted in order of the production number. The solid circle at 14th position in each plot corresponds to the short-layered magnet.

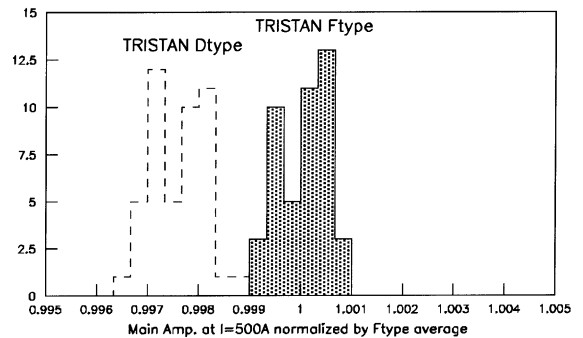


Fig. 3. Distribution of the amplitude (normalized by the TRISTAN F-type average) for the main component at $I = 500$ A. The upper and lower peaks correspond to those for the TRISTAN F-type and D-type magnets, respectively.

Table 8
Magnetic field measuring results for the dipole and wiggler magnets

	Type of magnets	B_{design} (T)	I_{max} (A)	L_{lam} (m)	L_{eff} (m)	B_{meas} (T)	$\Delta BL / \langle BL \rangle \times 10^{-4}$
LER	B	0.848	1250×32	0.76	0.8876	0.83616	4.724
	B1c	0.52	1000×24	2.1	2.2273	0.52697	3.514
	BV	0.20	500×18	1.2	1.3561	0.20523	
	BS	0.21	500×20	0.3	0.4085	0.21994	
HER	B	0.30	840×10	5.804	5.9006	0.29974	3.234
	BS1	0.048	10×150	2.8			
	BsFL	0.214	500×12	1.14	1.2393	0.21473	
	BsFR	0.339	500×32	0.76	0.8935	0.35205	
LER	Wig	0.77	944.4×36	0.75	0.6939 (3.34×10^{-4} Tm)	0.77056	11.68 (6.395)

In the row for the wiggler magnets, values in parenthesis are BL , integrated B all through the magnetic gap of the wiggler magnets. Values not in parenthesis are $|B|L$, the sum of absolute integrated B for each pole.

Table 9
Magnetic field measuring results for quadrupole and sextupole magnets-I

	Type of magnets	B'_{design} (T/m)	I_{max} (A)	L_{lam} (m)	L_{eff} (m)	B'_{meas} (T/m)
LER	QA-I	10.2	500	0.4	0.45944	10.321
	QA-II	10.2	500	0.4	0.45899	10.329
	Qrf	6.32	500	0.5	0.58213	6.375
	Qk	0.73	200	0.2	0.29780	0.7163
HER	QA	8.5	500	0.762	0.82542	8.497
	QB	8.5	500/600	0.95	1.01551	8.507
	QS	12.7	500/600	0.5	0.55410	12.808
	QX	12.7	500	0.8	0.81259	12.840
	Qrf	6.32	500	1.0	1.07931	6.357
	Qk1	1.25	200	0.3	0.37986	1.2547
	Qk2	0.73	200	0.5	0.59312	0.7294
		B''_{design} (T/m ²)				B''_{meas} (T/m ²)
LER	SX	340	425	0.3	0.33580	330.89
	SxC	77.5	425	0.5	0.55277	78.037
HER	SxF	340	425	0.3	0.33580	330.89
	SxD	348	425	1.0	1.01913	352.75

Table 10
Magnetic field measuring results for the quadrupole and sextupole magnets-II

	Type of magnets	$\Delta B'L / \langle B'L \rangle$ $\times 10^{-4}$	$\Delta L_{\text{eff}} / \langle L_{\text{eff}} \rangle$ $\times 10^{-4}$	ΔX (mm)	ΔY (mm)	$\Delta \theta_{\text{med}}$ (mrad)
LER	QA-I	7.2	4.5	0.05	0.03	0.15
	QA-II	6.6	4.4	0.04	0.04	0.10
	Qrf	6.8	3.5	0.03	0.03	0.19
	Qk	7.1	7.0	0.05	0.07	0.44
HER	QA	6.0	4.4	0.04	0.07	0.17
	QB	5.0	4.2	0.05	0.06	0.22
	QS	5.5	3.8	0.05	0.04	0.10
	QX	4.9	6.0	0.06	0.05	0.22
	Qrf	7.5	2.0	0.06	0.01	0.22
	Qk1	3.1	4.2	0.03	0.03	0.27
	Qk2	2.1	2.7	0.04	0.01	0.15
		$\Delta B''L / \langle B''L \rangle$ $\times 10^{-4}$				
LER	SX	13.0	9.1	0.03	0.04	0.34
	SxC	3.3	3.1	0.02	0.02	0.07
HER	SxF	13.0	9.1	0.03	0.04	0.34
	SxD	8.1	8.3	0.04	0.04	0.28

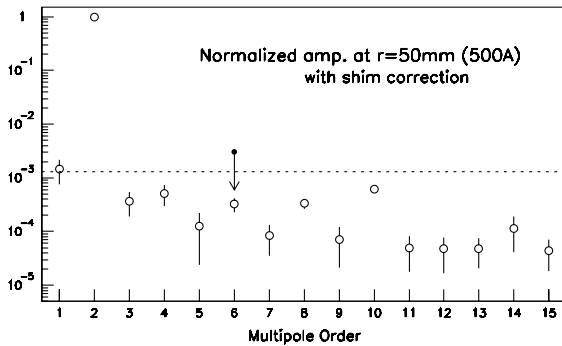


Fig. 4. Normalized multipole amplitude for the LER-QA magnets plotted as a function of multipole order. The solid circle indicates the amplitude for sixth multipole before the shim correction. Requirement for the lowest allowed multipole $n = 6$ is indicated by a dotted line. The error bars indicate one standard deviation of each multipole.

tion is made for the LER-B magnets to adjust the BL [8]. The pole-end shim-correction is also made for LER-QA, HER-QS and HER-QX type magnets to reduce the allowed higher order components [6]. An example for the LER-QA magnets is shown in Fig. 4. The amplitudes for $n = 6$ component before and after a shim-correction are shown by the solid circle and open circle in the figure, respectively. The amplitudes for the other components after a shim-correction are also shown by the open circles. The amplitude of the higher order components in each type of magnets is small enough compared with the tolerances listed in Table 1.

6. Installation and alignment

Preparation for the KEKB magnet installation was started in October 1995. At first, the level of the TRISTAN quadrupole magnet center was transferred to beam-level markers installed on the tunnel wall; 108 beam-level markers were installed for the KEKB magnets at an interval of about 30 m. Later, this number was increased to 202 by installing extra markers between. These beam-level markers were surveyed during the period from February to June 1996, and the inclination of the tunnel was found. The difference

between the highest point at the Tsukuba area and the lowest point in the east arc is about 13 mm. Then, the height of a beam-level marker was measured from the top surface of several base plates for the TRISTAN quadrupole magnets at the highest point, and was found to be lower than the designed value by 10 mm. The point higher than the highest beam-level marker by 10 mm is thus taken as the KEKB beam-level. The deviation for each beam-level marker from this KEKB beam-level is written on slips pasted on the wall near to the corresponding markers, and the height of each beam-level marker is corrected by this deviation when it is used as a reference. In this way, the magnets are aligned so as to be level. Since the first survey, the level of the markers has been surveyed almost once a year. The results are shown in Fig. 5. After a survey in September 1997, the beam-level markers were adjusted to beam level because mistakes were easily introduced in making such a big offset from the markers. A plot was made separately for deviations (a) before and (b) after this adjustment. It can be seen from this plot that the south part of the tunnel is sinking compared with the Tsukuba area at a speed of about 2 mm/year. This movement of the ground has resulted in an accumulated settlement of 13 mm/km during 9 years of the TRISTAN operation, where 1 km is the diameter of the accelerator ring.

Actual construction of the KEKB ring was started in January 1996, soon after termination of the TRISTAN operation. All of the accelerator elements were carried out and the tunnel was cleaned. The surface of the 1.2 m wide passage was repainted with 2 mm thick epoxy paint for Hovercraft-type magnet transporters. The center markers installed on the tunnel floor for the TRISTAN quadrupole magnets were used as KEKB monuments for the horizontal position. It is convenient for the KEKB magnet alignment to use the TRISTAN markers because a precision of ± 10 mm for the ring circumference is required and the circumference along these TRISTAN markers was well known from the timing of the beam circulation. It would be quite hard to achieve this 3 ppm precision ($= 10$ mm/3 km) without these well-known markers. From the

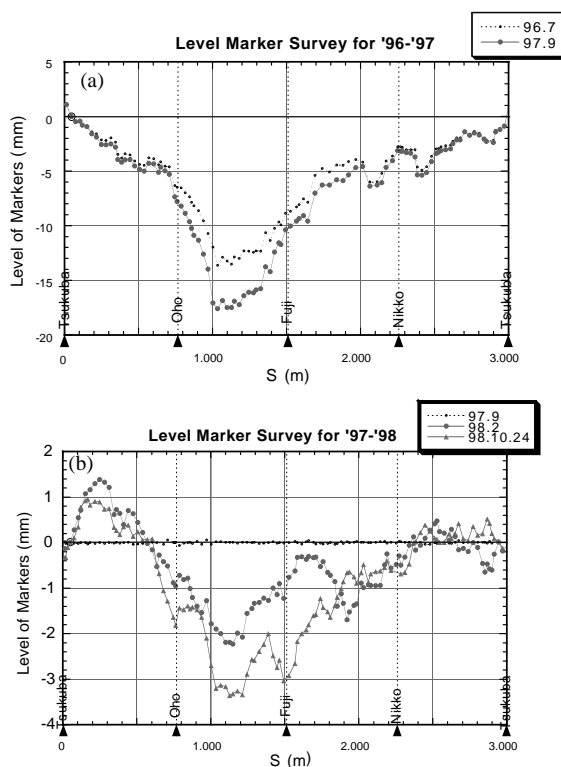


Fig. 5. Levels of beam-level markers. The beam-level markers were installed transferring center height of the TRISTAN quadrupole magnets, and they were adjusted to be level in September, 1997. Figs. (a) and (b) show the results before and after this adjustment, respectively. The dotted line and the solid line in figure (a) stand for the survey results in July, 1996, and September, 1997, respectively. The solid circles and the solid triangles in figure (b) stand for the survey results in February, 1998, and October, 1998, respectively.

commissioning of KEKB beams the errors for the circumference were found to be +5.1 mm for LER and +5.4 mm for HER, respectively. These errors are within the tolerance of ± 10 mm. The center markers of the TRISTAN quadrupole magnets were surveyed by a laser tracker, modern three-dimensional position measuring equipment having a capability of automatic target chasing, for 4 months from April to July 1996. However, because the air conditioner was turned off during this survey, a problem occurred, as described later. In any case, the beam lines for LER and HER were then drawn on the tunnel floor using the position

markers as reference. Points (called B points) on the KEKB beam lines, which are 100 mm from the surface of the end plates of bending dipole magnets, were plotted first. The beam lines were then drawn by connecting these B points, and the center position for quadrupole and sextupole magnets was plotted by having their distance from B points. The center points for the main dipole magnets were plotted in the middle of both side B points, having the offset from the connected line. Installation of base plates was begun in December 1996. Because it is time consuming and expensive to remove the TRISTAN base plates, KEKB magnet base plates were installed over the TRISTAN ones. Thus, the available height for the base plates plus the magnet supports is less by 30 mm, the thickness of the TRISTAN base plates, than that in TRISTAN. In installing these base plates, the distance between the top surface of the magnet base plates and the beam level was to be 825 mm in the arc section and 1425 mm in the straight section respectively. Because the KEKB rings were constructed in the existing tunnel, some base plates had to be installed across the tunnel expansion joint. In this case, one end had to be fixed and the other must be movable only along the beam direction.

The installation of magnets started in February 1997, just after a kick-off ceremony for magnet installation on February 26, 1997. Prior to the installation, magnet transporters were fabricated. It was not easy to design the magnet transporters, because the passage for transportation was very limited (1.2 m wide and 2.3 m high) and the speed should be fast enough to transport such a large number of magnets. There was thus almost no choice except for the Hovercraft-type transporters. The merits of this type are: (1) low height of a carrier, (2) low friction in movement, (3) compact guide, (4) almost no damage to the floor, and (5) quietness in movement. On the other hand, the demerit is a large electric power consumption of 15 kW in our case. A mechanism to stop it (especially the emergency stop) must be carefully considered because the friction of movement is so small that it is hard to stop. Also the surface of the floor must be smooth, and should not have any cracks. The passage was therefore repainted with a

special thick paint (as described previously). For the electric power supply, three-phase trolley lines of $200\text{ V} \times 200\text{ A}$ were installed under cable racks stretched from the inner-side wall (passage side). Two sets of Hovercraft-type magnet transporters were fabricated. A set consists of an electromotive tractor driven by DC 24 V batteries of 600 W, an air compressor with an output of $7\text{ kg/cm}^2 \times 2.3\text{ m}^3/\text{min}$ and two carriers. Each carrier is equipped with two 3 m long guiding beams which can rotate in the horizontal plane. Another hooking beam is installed across these guiding beams to hook magnets and move along the guiding beams. This set of beams is lifted up and down by a hydraulic system. The guiding beams are folded when the transporter is running, and are expanded toward the magnet position when they arrive at the target position. The expanded beams are supported at their ends by supporting poles waiting at the corresponding position. The height of the poles is changed by a hydraulic system synchronized with the change in the height of the guiding beams. Two carriers are used to transport the longest 6 m HER-B magnet, and one carrier for the other magnets. In some place the length of the guiding beams is not sufficient. In that case, a magnet is handed over from the transporter onto a movable table waiting. Upon receiving a magnet, the movable table raises its height by a hydraulic system, moves along guide rails and lowers the

magnet onto waiting magnet supports. Fig. 6 shows the scene for installing a HER-B magnet.

The alignment work started in early October 1997, from the outer ring in the north arc. The alignment was performed for the outer ring first using the horizontal position monuments on the floor and the beam-level markers on the wall as reference. After finishing the alignment for the outer ring, the inner ring was aligned using the magnets in the outer ring as reference. Two fiducial bases were installed along the center axis on the top surface of each magnet. In the center of the base, a hole was drilled to hold an alignment target, a Taylor Hobson optical target, for the telescope or a cat's-eye mirror for the laser tracker. The surface of fiducial bases is machined flat and its tilt from the median plane of a magnet is required to be smaller than $\pm 0.1\text{ mrad}$. The diameter and the center position of the hole are drilled with a high precision of $\pm 10\text{ }\mu\text{m}$ and $\pm 0.1\text{ mm}$, respectively. The alignment of the level and horizontal position of the magnets is performed by measuring an alignment target inserted into these fiducial holes. In the arc section a laser tracker (Leica SMART 310), a leveling telescope (Wild N3) and a Carl Zeiss level are used to measure the horizontal position, level and tilt, respectively. Later, another laser tracker (Leica LT500) is added to speed up the alignment work. On the other hand, a different method is used for the 200 m long straight section except for the Tsukuba area. In the Tsukuba area, the same method is used as the arc section because the beam lines are winding because of LER local chromaticity correction. The stretched-wire method surpasses the two-dimensional positioning method using a laser tracker in aligning magnets on the straight. Thus, in the straight section a stretched-wire system is adopted to measure the deviation of the magnet position from the line connecting the magnets located at both ends of the straight section. These end magnets are aligned in the preceding arc alignment. The stretched-wire system uses a semiconducting wire of 0.6 mm diameter and capacitance-type wire position measuring equipment. The distance from the end magnet is measured by a Leica ME5000 Mekometer. The level and tilt are measured by using



Fig. 6. A picture of a scene of magnet installation. A 6 m long HER-B magnet is handed over from the magnet transporter to the movable table to be installed to assigned position.

the same equipment as that for the arc section, a Wild N3 leveling telescope and a Carl Zeiss level.

A problem was found in the alignment results for the outer ring in the north and west arcs. A survey performed after the alignment showed large and systematic errors in the horizontal position along the beam line. The error was large at the position of expansion joints of the tunnel and small at the middle. This was caused by a room temperature variation. At the time of the survey for the horizontal position monitors, the air conditioners were turned off, and the temperature sometimes showed as low as 18°C. In autumn 1996, the air conditioners were turned back on and the room temperature had been controlled around 24°C since then. This temperature difference resulted in a length variation of the 65 m long tunnel section by some millimeters. This is the cause of such a large alignment error. The monuments were surveyed again in the south and east arcs, where the alignment was not yet started. In the north and west arcs, the horizontal positions of the magnets in the outer ring were corrected according to the results of the error analysis. After finishing the alignment for both of the outer and inner rings, the horizontal positions of the magnets were surveyed. Any errors larger than 0.1 mm were corrected. Ultimately, the alignment work converged in three or four repetitions in the north and west arcs and in two in the other places.

Figs. 7 and 8 show an example of the results of the alignment in the west arc. The solid and dotted lines in Fig. 7 show the alignment errors in the radial direction and the direction along the circumference, respectively. In this figure (a) is for the LER and (b) for the HER. Fig. 8 shows histograms for these errors. The alignment tolerances are given in Table 11, and a summary of the alignment errors is given in Table 12. Because an alignment was carried out independently in each section the kink between the beam line in an arc section and that in a straight section was of concern. By surveying the positions of the magnets, it was found that kinks in 8 places were less than 0.09 mrad, and that all of them were tolerable. Details of the magnet alignment are reported in Ref. [9].

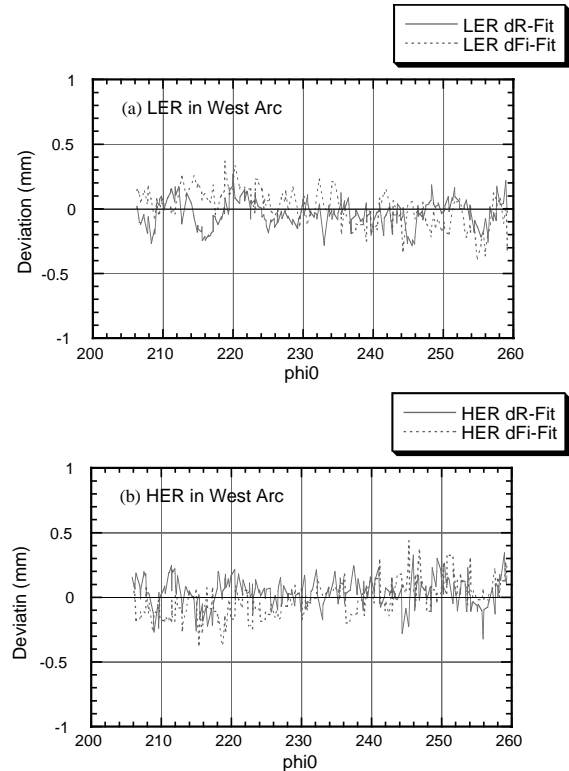


Fig. 7. Results of magnet alignment in the west arc (a) for LER and (b) for HER. Vertical axis shows deviation of magnet position from the designed value. Deviations in radial direction is shown by the solid lines and that along circumference is shown by the dotted lines.

7. Power supply system

Although much more power supplies are required for KEKB than for TRISTAN, they must all be accommodated in the existing buildings, and all cables must be installed on the existing cable racks. For the magnet power supplies of the main ring, there are four large buildings (D2, D5, D8 and D11) annexed to the four TRISTAN experimental halls and four small buildings (D3, D6, D9 and D12) located between the large ones along the circumference of the accelerator ring. In order to accommodate all of the power supplies in these PS buildings, switching regulators, a new type of regulators, are adopted as medium and small power supplies. The switching regulators for medium power supplies use the Insulated Gate

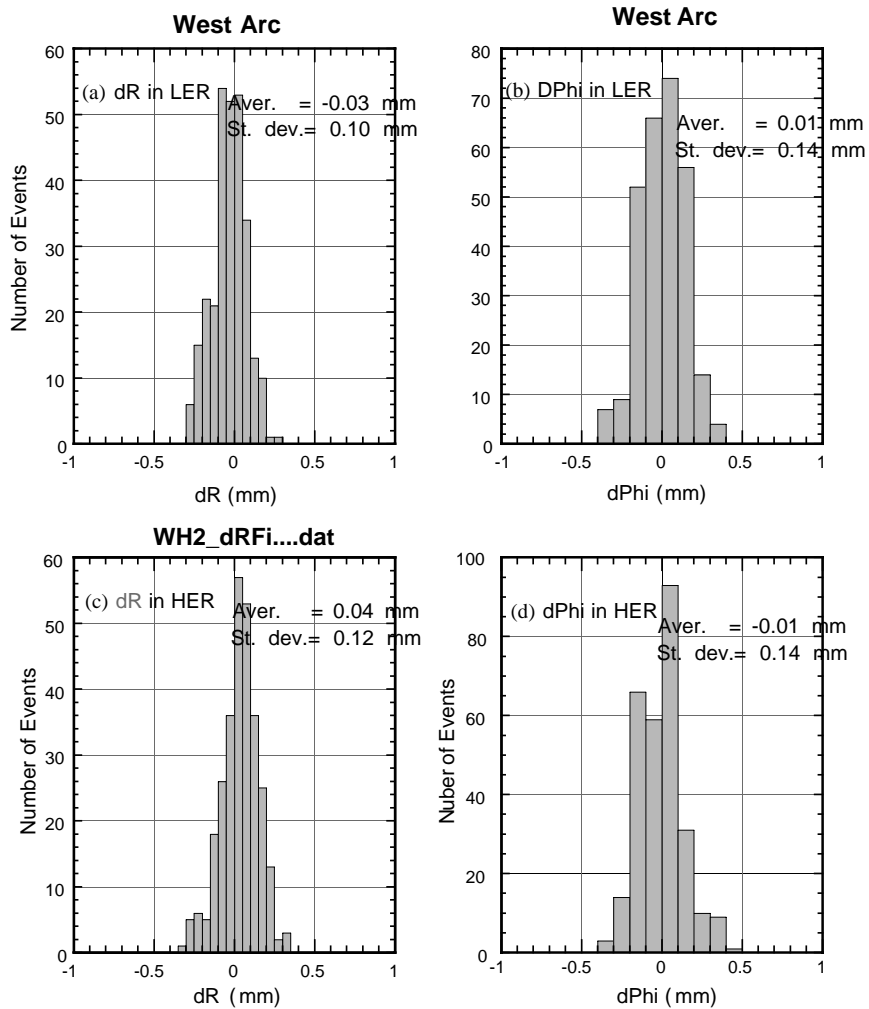


Fig. 8. Results of magnet alignment in the west arc (a) and (b) for LER and (c) and (d) for HER. (a) and (c) show deviations in radial direction, dR . (b) and (d) show deviations along circumference, $d\phi$.

Table 11
Tolerances for alignment errors

Horizontal position	
Transverse direction	± 0.15 mm
Along the beam line	± 0.5 mm
Height	± 0.15 mm
Tilt	± 0.1 mrad
Circumference	± 10 mm

Bipolar Transistor (IGBT) modules with a switching frequency of about 20 kHz. Those for small power supplies use MOS-FETs with a switching

frequency of about 100 kHz. The numbers of small power supplies and medium ones are 1841 and 362, respectively. Most of the small power supplies are for steering dipole magnets and correction coils of the main magnets. Eight large power supplies have been recycled from TRISTAN, which use the thyristor regulators plus active filters. The other 20 large power supplies of thyristor plus transistor dropper type have been newly fabricated. Each of the large and medium power supplies feed current to some number of magnets which are connected in series. The total number of power supplies is 2231. The types of power supplies are summarized

in Table 13. In order to use the existing cable racks, the current fed to magnets is designed to be as small as possible.

The specifications of the power supplies were fixed before the end of 1996. The first lot was ordered in June 1997, and the delivery was completed in July 1998.

The tolerances for the power supplies are listed in Table 14. Those for the dipole and quadrupole magnets are not easy to be satisfied. It is hard for power supplies to remain stable throughout the year, because the PS buildings are not equipped with air conditioners and the room temperature becomes about 10°C in the winter and reaches about 40°C in the summer. Therefore, the components which are sensitive to a temperature variation must be placed in temperature-controlled

containers. The recycled large power supplies already had thermostatic chambers, and only the DC Current Transformers (DCCTs) and some other small elements were replaced by new ones. In the newly fabricated large and medium power supplies, the Digital to Analog Converters (DACs), buffer and feedback amplifiers and burden registers are placed in small thermostatic containers whose inner temperature is controlled by Peltier modules. The inner temperature is controlled within $\pm 0.5^\circ\text{C}$. Special attention was paid to selecting elements which play an important role in realizing high precision, such as burden registers for large and medium power supplies, shunt registers for small power supplies and DCCTs. The DACs were baked at 85°C for about 20 hours beforehand to reduce long-term drift.

A block diagram of the power supply system is shown in Fig. 9. The power supply system is controlled by records written in EPICS. The control records and data are stored in local CPUs, called IOCs, installed in VME subracks in each PS control room. Commands are transferred through the Ethernet from the central computer down to IOCs. The status of the power supply system, interlock status and monitoring data for currents

Table 12
Summary of standard deviations of alignment errors

Area	LER		HER	
	Δ_R	Δ_ϕ	Δ_R	Δ_ϕ
Tsukuba	0.08	0.09	$\leftarrow \text{LER} + \text{HER}$	
North arc	0.09	0.12	0.10	0.10
West arc	0.11	0.14	0.12	0.14
South arc	0.09	0.10	0.11	0.10
East arc	0.10	0.17	0.11	0.16
All arc sections	0.10	0.14	0.11	0.13
Nikko	0.01	0.27	0.03	0.11
Fuji	0.01	0.27	0.03	0.19
Oho	0.04	0.08	0.03	0.14
All straight sections	0.02	0.22	0.03	0.15
Tolerances	0.15	0.50	0.15	0.50

Unit is millimeters. D_R and D_ϕ stand for errors in radial direction and along circumference, respectively.

Table 14
Tolerances for current stability and ripple content

Type of magnets	Current stability (P-P) (ppm/year)	Ripple content rate (P-P) (ppm)
Dipole magnets	100	10
Quadrupole magnets	100	10
Sextupole magnets	500	500
Steering magnets	500	50

Table 13
Power supplies for KEKB

Type	Regulator mode	Power (kW)	Number
Large PS recycled from TRISTAN	SCR + active filter	460–900	8
Large PS newly fabricated	SCR + transistor dropper	100–440	20
Medium PS	Switching of ~ 20 kHz	2–124	362
Small PS	Switching of ~ 100 kHz	<1	1841

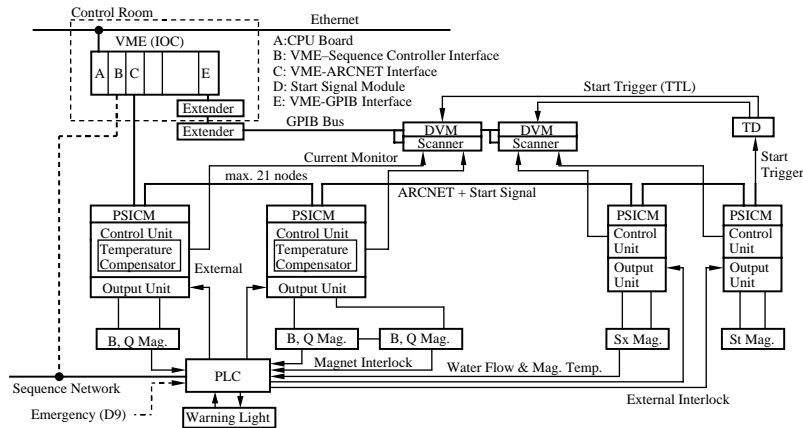


Fig. 9. Block diagram for the magnet power supply system for the KEKB main ring.

is transferred from IOCs up to the central computer. Communication between the IOC and Power Supply Interface Controller Modules (PSICMs) is made through a VME-ARCNET interface module, which has four ports and can handle 80 PSICMs (20 PSICMs/port). PSICMs are connected to each other by Attached Resource Computer NETWORK (ARCNET). The steering dipole magnets are required to be excited synchronously with each other to keep the beams circulating. The ARCNET serial bus uses a twisted pair cable. Another one used to deliver synchronized start pulses is installed along this ARCNET bus line. The synchronized start pulses, sent out by start signal modules installed in the VME subracks for other group, go directly to the VME-ARCNET interfaces, and are delivered to each PSICM through ARCNET. By adopting ARCNET instead of CAMAC, the cost for the control system is greatly reduced and high-speed synchronous control for the steering dipole magnet power supplies is achieved. All of the power supply IOC systems conduct the synchronous control for up to 8 steering dipole magnets at one time at a time interval of 5 s. The magnet power supply system has an IOCs in each PS control room (8 IOCs in total) and an extra one in the central control room for synchronous current setting.

The PSICM has two current setting modes, a constant slew rate mode and a wave-generator mode. In the former mode, the current is set linearly with a constant slew rate. In the latter

mode, the current setting is divided into small steps; the setting values for each step are calculated in the IOC according to the desired form, and these setting values are stored in the memory in the PSICM. The current setting for the steering dipole magnets is triggered by a synchronous start pulse. This can also be done in the asynchronous mode (called soft start) as the main magnet current setting. In sending the target value to the DAC, the raw data is once stored in the first buffer, and is then corrected according to the linear form extracted from the memory in the power supply. The corrected data is stored in a second buffer, and sent to the DAC. This is called double-buffer method, which is adopted to avoid having trimmers, such as variable registers, to adjust the gain and offset of the power supplies. Trimmers are one of the main sources of trouble and long-term drift. By using this double-buffer method, the precision for the current setting is improved from an order of ± 1000 ppm to ± 50 ppm, or better.

The output of DAC is fed to an feedback amplifier and then to a Pulse Width Modulator (PWM). The output from the PWM powers a magnet. The current fed to a magnet is detected by two DCCTs; one is for feedback and the other for monitoring. By having a monitoring DCCT, any malfunctioning of the whole feedback system, including the feedback DCCT, can be detected. The output from the feedback DCCT is fed to the feedback amplifier through a burden register and a buffer amplifier. The output from the monitoring

DCCT is also fed to a scanner, through a burden register and a buffer amplifier. The measuring data for the current are collected and digitized by a system consisting of a Digital Volt Meter (DVM) and a scanner, which are operated in the GPIB mode. The DVM-scanner systems are connected to the VME through a VME-GPIB interface. Up to 80 signals can be connected to a scanner. The digitizing is so fast that all current values of the 2231 power supplies can be read and stored in the IOC within 2 s. At present, the current values are read every 10 s to maintain a long life of the scanners. To realize a precision of ± 50 ppm, the read data are corrected according to the linear form in the IOC by extracting correction coefficients from the memory in the power supplies. Correction coefficients are obtained by comparing the data from each channel with the value obtained by a standard measuring set.

For synchronous excitation of the steering dipole magnets, information concerning delay in the excitation is necessary. Delay is caused by the electric time constant in the control modules, power cables and coils of the magnets. It is also caused by an eddy current induced in the beam pipe by a change in the magnetic flux. The beam pipe is made of aluminum in some part of the Tsukuba and Fuji straight section and of copper in other places. The delay caused by the eddy current

in the beam pipe is dominant, and it has been measured. By exciting a steering magnet with the sum of frequency harmonics, the spectrum of the magnetic field was measured on the surface of the beam pipe by using a Hall probe and a spectrum analyzer. From the amplitude drop for some frequency spectrum, the time response of the magnetic field in the steering magnet was obtained.

A block diagram of the interlock system is shown in Fig. 10. It is controlled by one CPU placed in the D8 PS building, which is called Programmable Logic Controller (PLC). Two optical fiber rings are installed along the circumference of the accelerator ring. One is for signal and command transfer, and the other for monitoring and display. A warning light system and interface modules are connected to an optical fiber link in each PS building. The interface modules receive interlock signals from magnets placed in each corresponding tunnel area, and transfer them to the PLC. These interlock signals are called external interlock signals, which consist of cooling water flow switch signals, magnet coil-temperature signals, warning light signals and an emergency stop signal. The emergency stop signal is sent out from the safety control system at the D9 control room and transferred to the magnet power supply interlock system through an interface module at the D9 PS building. Upon receiving an interlock

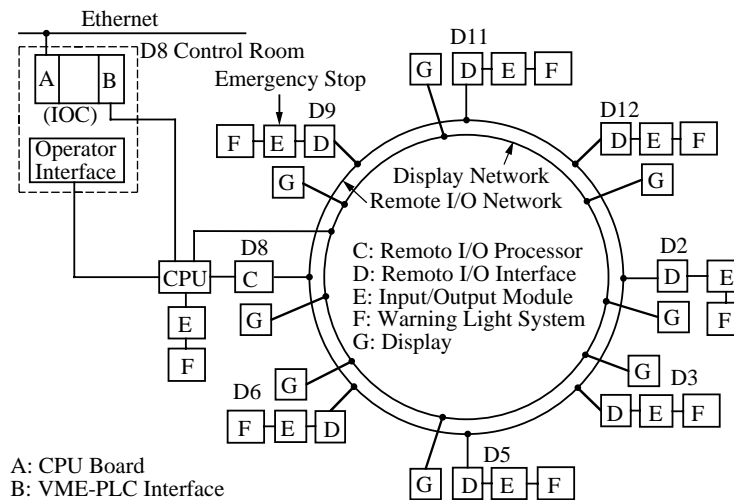


Fig. 10. Block diagram for the interlock system for the magnet power supplies.

signal through interface modules, the corresponding power supply turns off its power. The warning light systems turn on/off the warning lights by receiving turn on/off commands. The warning lights can be turned off locally. This local operation has the priority over remote commands for safety. After the warning lights are turned on, power supplies can set the current. When any warning light line is open during the operation, a warning light interlock signal is turned on. Any abnormal status of the power supplies also produces interlock signals, which are called internal interlock signals. They are detected by PSICMs, and are transferred to IOCs. The PLC is connected to the VME through a VME-PLC interface module installed in the VME subrack at the D8 PS control room. Through this connection, IOCs can read the status of the external interlocks, reset the interlock status and control on/off of the warning lights.

The details of the KEKB magnet power supply system are described in Refs. [10,11].

8. Summary

About 1600 main magnets (dipole, quadrupole, sextupole and wiggler magnets) and about 1700 steering dipole magnets were prepared for KEKB. Out of them, 119 dipole and 314 quadrupole magnets for the TRISTAN experiment were refurbished and used as HER main magnets. All other magnets were newly fabricated. The main dipole magnets are equipped with back-leg coils, and the quadrupole and sextupole magnets with correction coils. One-turn coils are installed to each magnetic pole of the main magnets as well to monitor the magnetic flux in the case of trouble. High precision is required on the magnetic field strength integrated along the beam direction and the field effective length. Special attention was paid to suppress the higher order multipole components. High precision is also required concerning the flatness, tilt and position of the fiducial bases on the magnets. The magnetic field integrated along the beam direction is measured for all magnets by using various types of field measuring equipment such as flip coils, rotating

coils, NMR and Hall probes. The distribution of the magnetic field along the beam direction is measured by short twin flip coils, and the field effective length is analyzed. The magnetic field quality is inspected strictly by this field measurement. The mechanical precision of the fiducial bases is also inspected by aligning magnets before starting a field measurement. Information on problems found in this field measurement are quickly fed back to the fabrication factory. All sextupole magnets are fixed on remotely controlled movers, which can adjust the position of magnets with a precision of 4 μm over a range of ± 2 mm.

Magnets were installed by using newly fabricated Hovercraft-type transporters, which fitted the narrow passage of the KEKB tunnel. A precision alignment of magnets was performed using modern instruments, like laser trackers, and standard ones, such as leveling telescopes and precision levels. In the straight section the stretched-wire method was used to align the magnets on the straight and the distance was measured by a Mekometer. The alignment was repeated two to four times until the alignment errors satisfied the tolerances.

A cooling water system for the magnets was constructed. Magnet cooling water is supplied from four cooling stations, each of which covers a quarter of the accelerator ring. Diaphragm-type water flow switches and bimetal-type coil-temperature switches protect magnets by setting interlock signals. Globe valves installed at the water inlet control the water flow. Opening of the globe valves and the interlock level of the water flow switches are adjusted by measuring the water flow by supersonic water flow meters. Since the improvement of air-evacuation system in the summer of 2000, there has been no power supply breakdown originating from water flow interlocks.

A magnet power supply system was constructed. In order to install all of the power supplies in the existing 8 PS buildings, compact power supplies had to be designed. Therefore, switching regulator type power supplies were adopted. There are 1841 small power supplies and 362 medium ones. Only 8 large power supplies of the thyristor plus active filter type were recycled from TRISTAN, and another 20 large power supplies of the thyristor

plus transistor dropper type were newly fabricated. PSICMs are connected to each other through the ARCNET. By correcting the current setting values in the PSICMs in the double-buffer mode, a precision of ± 50 ppm is achieved without using any trimmers. PSICMs are controlled by IOCs installed in VME subracks in each PS control room. The monitored current values are also corrected in the IOCs for the offset and the error in the gain of the system. A precision of ± 50 ppm has been achieved. Synchronous excitation for the steering magnets is required; the power supply system has this capability by utilizing synchronized start pulses. The interlock system has its own optical fiber link. Interlock signals from each magnet are transferred to the interlock system interface modules in the nearest PS building and delivered to the corresponding power supply through the interlock optical fiber link. The interlock system is controlled by a single CPU, called PLC, which is located in the D8 PS building, and communicates with the IOCs through the VME-PLC interface module.

The sextupole magnet movers, magnet power supplies and a part of the magnetic field measuring system are controlled by IOCs. The control software system is built within the framework of the EPICS.

Construction of these two rings took 5 years. Designing the magnets started in 1994, and their alignment was completed in November 1998.

Acknowledgements

The authors owe the successful accomplishment of this KEKB magnet system construction to the devoted work by many people from companies. We would like to thank Prof. Shin-ichi Kurokawa, the leader of the KEKB accelerator construction, and now the head of divisions of Accelerator Laboratory, for his continuous encouragement and help. We would also like to thank Mr. Yin Zhaosheng and other people of IHEP in Beijing and Prof. Nikolai S. Dikansky, Dr. Valeri V. Petrov and the people of their group of BINP in Novosibirsk for their effort in the fabrication of steering dipole magnets. Mr. Gordon B. Bowden

at SLAC helped us with precision sextupole magnet movers by giving us information about their cam shaft movers. Finally we would like to thank the staff who contributed to the KEKB accelerator construction for their cooperation.

References

- [1] National Laboratory for High Energy Physics, KEKB B-factory design report, KEK Report 95-7, August 1995.
- [2] Belle collaboration, Belle technical design report, KEK Report 95-1, April 1995.
- [3] TRISTAN project group, TRISTAN design report, KEK Report 86-14, March 1987.
- [4] G. Bowden, P. Holik, R. Wagner, Precision magnet movers for final focus test beam, SLAC-PUB-95-6132, June 1995.
- [5] A. Akiyama, S. Araki, J-I. Odagiri, T. Katoh, T. Kawamoto, I. Komada, K. Kudo, T.T. Nakamura, T. Naito, N. Yamamoto, KEKB control system: the present and the future, in: Proceedings of the 1999 Particle Accelerator Conference, New York, March 29–April 2, 1999.
- [6] K. Egawa, M. Masuzawa, Field measurement results of the KEK B-factory quadrupole and sextupole magnets, in: Proceedings of the 1999 Particle Accelerator Conference, New York, March 29–April 2, 1999.
- [7] K. Egawa, M. Masuzawa, Study of the magnetic coupling between quadrupole and dipole corrector magnets for the KEK B-factory, in: Proceedings of the 1999 Particle Accelerator Conference, New York, March 29–April 2, 1999.
- [8] K. Egawa, M. Masuzawa, Field measurements of the KEK B-factory dipole and wiggler magnets, in: Proceedings of the 1999 Particle Accelerator Conference, New York, March 29–April 2, 1999.
- [9] R. Sugahara, M. Masuzawa, Y. Ohsawa, M. Sakai, H. Yamashita, Installation and Alignment of KEKB magnets, KEK Preprint 99-131, November 1999; in: Proceedings of the 6th International Workshop on Accelerator Alignment (IWAA99), ESRF, Grenoble, France, October 18–21, 1999.
- [10] M. Yoshida, T. Kubo, A. Akiyama, T. Nakamura, S. Yamamoto, R&D and system for KEK B magnet power supply, KEK-PREPRINT-97-192, October 1997; in: Proceedings of the 11th Symposium on Accelerator Technology and Science, Hyogo, Japan, 21–23 October 1997.
- [11] A. Akiyama, T. Katoh, T. Kubo, S. Kurokawa, T.T. Nakamura, M. Yoshida, Magnet power supply system for KEK B accelerator, KEK-PREPRINT-98-115, August 1998; in: Proceedings of the Sixth European Particle Accelerator Conference (EPAC 98), Stockholm, Sweden, 22–26 June 1998.